

## SHAKING TABLE TEST OF SOIL LIQUEFACTION IN SOUTHERN YOGYAKARTA

Lindung Zalbuin Mase<sup>1\*</sup>

<sup>1</sup>*Department of Civil Engineering, Faculty of Engineering, University of Bengkulu  
WR. Supratman. Rd, No.2, Kandang Limun 38371, Muara Bangkahulu, Bengkulu City, Indonesia*

(Received: November 2016 / Revised: May 2017 / Accepted: July 2017)

### ABSTRACT

On 27 May 2006, a 6.3 Mw earthquake hit Yogyakarta Special Province, Indonesia. This earthquake triggered a unique phenomenon, i.e., liquefaction. In order to learn from that earthquake event, an intensive study based on an experimental test of liquefaction potential using a shaking table was conducted. This study focused on the sandy soil in southern Yogyakarta, i.e., Opak River Watu, where liquefaction events occurred in 2006. Dynamic loads with accelerations from 3 to 4 m/s<sup>2</sup>, vibration frequencies from 1.4 to 1.8 Hz, and vibration times of 8, 16, and 32 seconds were applied. All dynamic loads were combined to observe the liquefaction mechanism, time to start liquefaction, time to start dissipation, and liquefaction duration. The results show that liquefaction can potentially occur in the sandy soil of Opak River Watu. The applied load strongly influences the potential for liquefaction, time to start liquefaction, time to start dissipation, liquefaction duration, and excess pore pressure ratio.

*Keywords:* Dynamic load; Earthquake; Liquefaction; Sandy soil; Shaking table

### 1. INTRODUCTION

On 27 May 2006, an earthquake with a magnitude of 6.3 Mw hit Yogyakarta Special Province. This earthquake produced some liquefaction events, such as lateral spreads and sand boils. In order to learn from the events, many researchers studied liquefaction in Yogyakarta Special Province, starting by performing empirical analyses based on secondary data, such as a CPT (cone penetration test) and an SPT (standard penetration test).

Yogatama et al. (2013) studied the potential for liquefaction based on the Liquefaction Potential Index (LPI) proposed by Iwasaki et al. (1982). The result showed that the high to very high potential areas for liquefaction were in the southern and eastern parts of Yogyakarta Special Province. A microzonation map from the Yogatama et al. (2013) study is presented in Figure 1. Mase et al. (2013) conducted an experimental study of soil liquefaction using a shaking table test. Their study focused on the eastern part of Yogyakarta, i.e., Imogiri. According to the Yogatama et al. (2013) study, Imogiri was categorized as a high potential area for liquefaction during the 2006 earthquake. In the study, Mase et al. (2013) considered the acceleration ( $a_{max}$ ) distribution studied by Fathani et al. (2008) and the Seismic Design Code of Indonesia (SNI-03-1726-2010). In Fathani et al. (2008), accelerations were applied at a vibration frequency ( $f$ ) of 1.6 Hz with a vibration time of 32 seconds. Mase (2017) performed an experimental study using a shaking table in the same area as that of the study performed by Mase et al. (2013). In the 2017 study, Mase (2017) applied the same variations in acceleration ( $a_{max}$ ) as Mase et al. (2013) had used. In addition, in the 2017 study, a vibration frequency of 1.8 Hz effect to the

---

\*Corresponding author's email: lindungmase@yahoo.co.id, Tel. +62-736-21170, Fax. +62-736-22105  
Permalink/DOI: <https://doi.org/10.14716/ijtech.v8i4.9488>

liquefaction potential, which was performed for various vibration times, i.e., 8, 16, and 32 seconds, was considered. In general, both experimental studies' results confirmed the previous empirical study conducted by Yogatama et al. (2013), in which Imogiri sands were categorized as a high potential area to undergo liquefaction. To progress beyond the previous studies, our experimental study was performed to observe the soil liquefaction mechanism, especially for the site experiencing liquefaction in 2006. In keeping with previous studies, the Opak River, located in the southern part of Yogyakarta, was studied, i.e., the Watu area, which had been categorized as an area with a very high potential for undergoing liquefaction.

In this study, the effect of dynamic load (following the study of Fathani et al., 2008), the effect of vibration frequency, and the effect of vibration time are explored in this study in order to observe the stages of liquefaction, such as the time to start liquefaction, the time to start dissipation, the liquefaction duration, and the maximum excess pore pressure ratio ( $r_u \max$ ). In order to obtain a clearer interpretation of liquefaction behavior on sandy soils, the results were also compared with those from the previous studies conducted in the same region by Mase et al. (2013) and Mase (2017). In general, this study is expected to provide a better understanding of the liquefaction potential in Southern Yogyakarta from an experimental standpoint.

## 2. STUDY AREA AND PRELIMINARY INVESTIGATION

This study focused on Opak River Watu, Southern Yogyakarta (Figure 1). The Watu sandy soil was sampled to investigate its physical properties (Table 1). In general, the soil sample was categorized as poor graded sand (SP) based on USCS (Unified Soil Classification System), with  $C_u$  and  $C_c$  values of 3.4 and 1.4 respectively. A rough estimation based on grain size distribution was also performed (Figure 2). For Figure 2, the rough prediction of liquefaction potential based on grain size distribution was performed by comparing the sample grain size distribution to the range of liquefiable grain size suggested by Tsuchida (1970). The grain size comparison showed that the soil sample was very vulnerable to liquefaction.

## 3. EXPERIMENTAL SETUP

The experimental test was conducted by a shaking table machine that belonged to the Cultural Heritage Preservation Agency of Prambanan Temple (Figure 3). The machine had a rigid platform for the soil sample container, with a maximum capacity of two tons. The shaking table was horizontally driven by an actuator. The maximum vibration frequency was 5.5 Hz and the maximum acceleration was  $12.5 \text{ m/s}^2$ . The container used in this study was a drum 60 cm in diameter and 80 cm in height. The container also had a circular plate for covering the top of the soil sample when the dynamic test was performed.

Some sample preparation steps were performed before test. First, the container was filled with distilled water up to 10 cm from the bottom. Next, the container was filled with sand, using a sieve filter with a mesh of 2 mm. Air bubbles appearing from the sample were removed. The previous steps were repeated until the expected height of 60 cm for sample was reached. Furthermore, the sample in container was left for at least two hours to ensure that the sample was totally saturated. After this step, the water overlaying the sample was removed. For the last sample preparation step, the circular plate was put on the soil deposit to ensure that there was no drainage path when the pore water pressure built up.

Prior to testing, the initial excess pore water pressure was recorded. Furthermore, The shaking table machine was prepared for the dynamic load. In this study, the dynamic load had three major variables, i.e., acceleration, vibration frequency, and vibration time. The accelerations were varied as  $3 \text{ m/s}^2$ ,  $3.5 \text{ m/s}^2$ , and  $4 \text{ m/s}^2$ . These values were taken from the Fathani et al. (2008) and Mase et al. (2013) studies. The vibration frequencies of 1.4, 1.6, and 1.8 Hz were

applied. These values were used since there was no accurate information on the 2006 ground motion frequency. However, according to Kusumawardhani (2014), the strong earthquakes triggering liquefaction had vibration frequencies of 0.5 to 2.5 Hz. The vibration times for the dynamic test were 8, 16, and 32 seconds. These values were drawn from the estimation of vibration time of various earthquakes' magnitude observed by Chang and Krinitzky (1977), for earthquake epicenters of less than 10 km. This recommendation was appropriate for the study area located about 10 km from the 2006 earthquake source. The variations in dynamic load are summarized in Table 2.

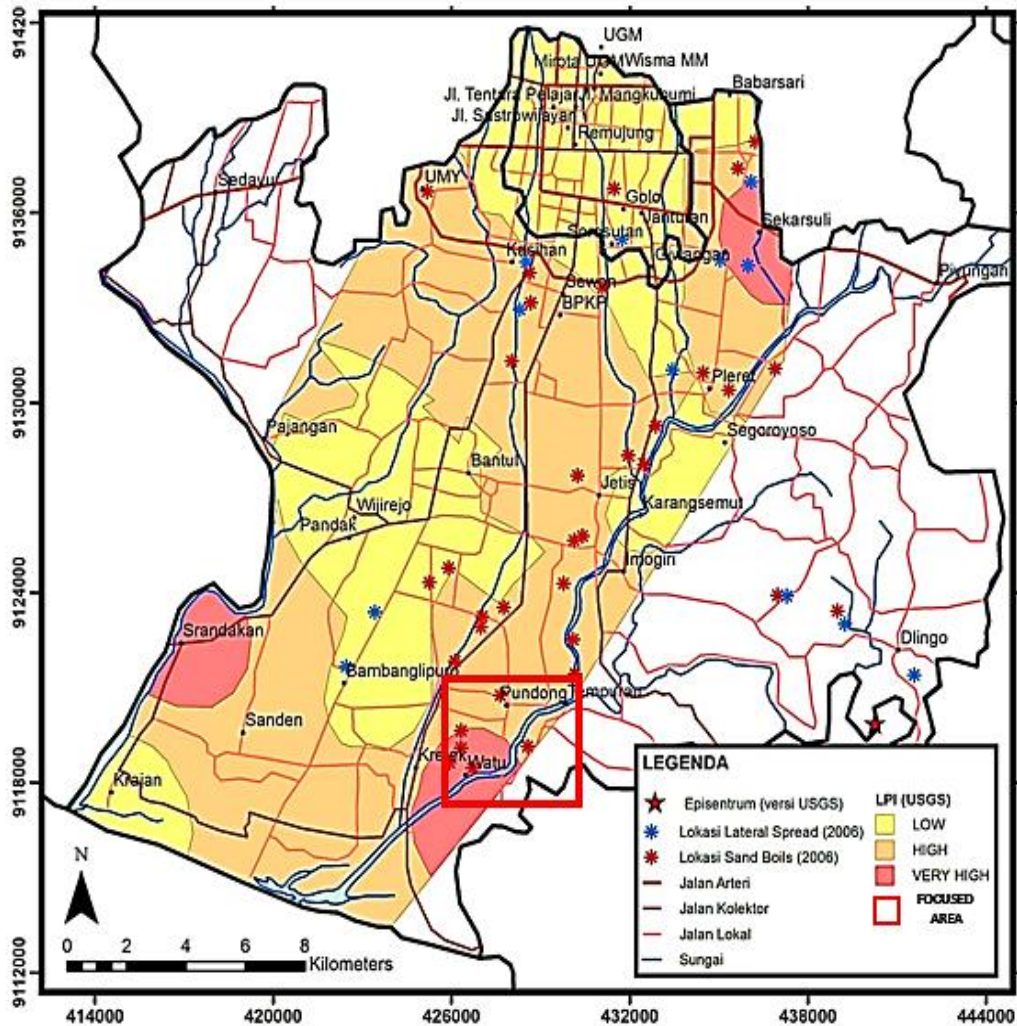


Figure 1 Study area and LPI map (Yogatama et al., 2013)

The excess pore water pressure was measured by pore pressure transducers that were installed at heights of 15, 30, and 45 cm from the soil surface. In this study, excess pore water pressure ( $\Delta u$ ) was measured for 60 seconds. To investigate liquefaction, excess pore water pressure was then compared with initial effective stress ( $\sigma'_v$ ) to obtain excess pore pressure ratio ( $r_u$ ) (liquefaction parameter). Liquefaction occurs if the  $r_u$  is more than or equal to 1 (Casagrande, 1936). This parameter has also been used by several researchers, such as Gupta (1977), Singh et al. (2008), Mase (2013), Mase et al. (2013), Laia (2014), and Komaji (2014) in performing a liquefaction potential study using a shaking table.

This study is composed of two experiment types. The first is the experimental test of the soil deposit under the dynamic loads listed in Table 2. This type is called *primary shaking*. The

second is the experimental test of the soil deposit that underwent primary shaking. For the second experiment, the dynamic loads listed were applied again (*secondary shaking*) to check the possibility of re-liquefaction. In the second experiment, the set-up steps were redone as in the first experiment.

In this study, the results of primary shaking are compared with those of the previous studies performed by Mase et al. (2013), who studied the liquefaction potential of Imogiri sand under a frequency of 1.6 Hz and a vibration time of 32 seconds, and by Mase (2017), who studied the Imogiri sandy soil liquefaction potential under a frequency of 1.8 Hz and various vibration times of 8, 16, and 32 seconds.

In this study, the liquefaction stages, which were compared to those in the above studies, were initial time of liquefaction, initial time of pore pressure dissipation, liquefaction duration, increase in percentage of liquefaction duration, and  $r_u \max$ . For the second experiment, the decrease in  $r_u \max$  was reported.

Table 1 Physical properties of Watu sand

Physical Properties	Notation	Value	Unit
Soil Classification (USCS)	SP	-	-
Uniformity Coefficient	$C_u$	3.4	-
Curvature Coefficient	$C_c$	1.4	-
Moisture Water Content	$w$	25	%
Bulk Density	$\gamma_b$	16.4	kN/m <sup>3</sup>
Dry Density	$\gamma_d$	14.1	kN/m <sup>3</sup>
Saturated Density	$\gamma_{sat}$	18	kN/m <sup>3</sup>
Specific Gravity	$G_s$	2.7	-
Maximum Void ratio	$e_{maks}$	0,99	-
Minimum Void ratio	$e_{min}$	0,58	-
Degree of Saturation	$S$	68	%
Relative Density	$R_D$	26	%

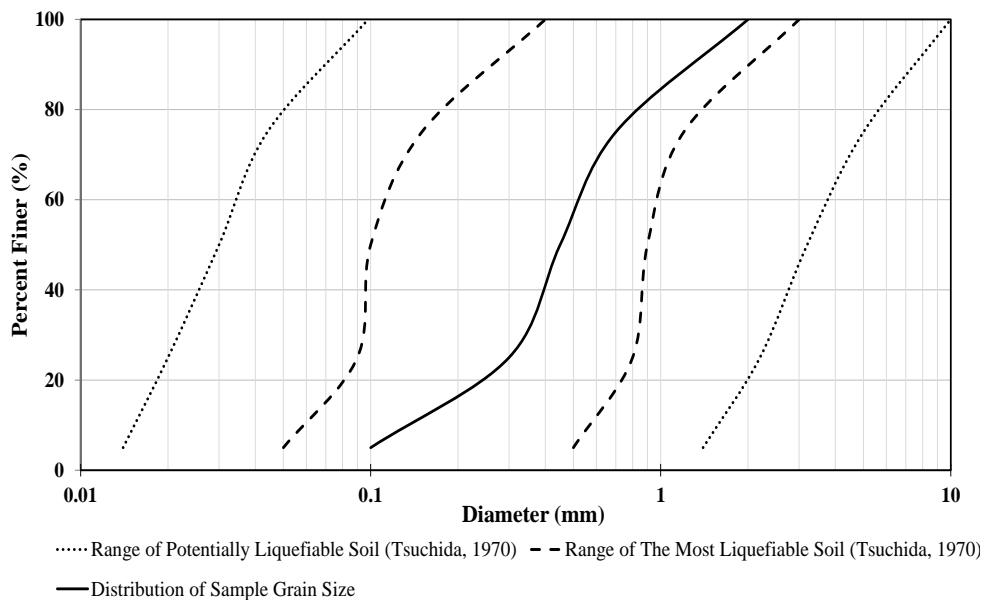


Figure 2 Liquefaction criteria based on grain size distribution

## 4. RESULTS AND DISCUSSION

### 4.1. Excess Pore Pressure Ratio ( $r_u$ )

During the test, the pore pressure transducer installed at a height of 15 cm and 45 cm didn't work well. Therefore, only the excess pore water pressure results measured by the pore pressure transducer at a height of 30 cm are reported in this study.

The interpretation of  $r_u$  under various vibration durations are presented in Figures 4 to 6. Figure 4 shows  $r_u$  for an acceleration of  $3 \text{ m/s}^2$ . The acceleration of  $3 \text{ m/s}^2$  with a vibration frequency ( $f$ ) of 1.8 Hz results in the highest excess pore water pressure among the dynamic loads of  $3 \text{ m/s}^2$ . In Figure 5, a similar trend is observed. The highest dynamic load, i.e.,  $3.5 \text{ m/s}^2$  with a vibration frequency of 1.8 Hz, resulted in the higher  $r_u$  compared with other  $3.5 \text{ m/s}^2$  loads.

Figure 6 represents  $r_u$  due to an acceleration of  $4 \text{ m/s}^2$  with variations in vibration frequency. Similarly to the previous result, the dynamic load plays an important role in determining  $r_u$ . In Figure 6, the  $r_u$  *max* resulted under an acceleration of  $4 \text{ m/s}^2$  with a vibration frequency of 1.8 Hz. Compared with the previous results,  $r_u$  in Figure 6 is the highest. In general,  $r_u$  depends on the applied load. The combination of higher acceleration and higher vibration frequency has an important role in determining  $r_u$ .

For the vibration time, it can be also observed in each figure that the  $r_u$  tends to be higher when the vibration time increases. The longer duration possibly increases the pore water pressure. When the duration increases, the excess pore water pressure tends to concentrate at the liquefaction threshold, i.e.,  $r_u \geq 1$ . This accumulated energy generates the higher  $r_u$ .



Figure 3 Shaking table machine and container used in this study

### 4.2. The Time to Start Liquefaction

The initial time of liquefaction is presented in Figure 7. In general, the initial time of liquefaction depended on the dynamic load applied. A higher dynamic load meant a shorter initial time of liquefaction. The higher dynamic loads produced higher energy, which makes it possible to generate pore water pressure that reaches or passes the initial effective stress.

Vibration time does not significantly influence the initial time of liquefaction. The same dynamic load applied at different vibration times generates the same initial time of liquefaction. However, as presented in Figures 4, 5, and 6, the vibration time tend to influence  $r_u$  under liquefied conditions ( $r_u \geq 1$ ). This phenomenon seems to influence the duration of liquefaction and the time to start dissipation.

Table 2 Dynamic loads applied in this study

Acceleration (m/s <sup>2</sup> )	Vibration Frequency (Hz)	Vibration time (s)
3.0	1.4	8
3.0	1.4	16
3.0	1.4	32
3.0	1.6	8
3.0	1.6	16
3.0	1.6	32
3.0	1.8	8
3.0	1.8	16
3.0	1.8	32
3.5	1.4	8
3.5	1.4	16
3.5	1.4	32
3.5	1.6	8
3.5	1.6	16
3.5	1.6	32
3.5	1.8	8
3.5	1.8	16
3.5	1.8	32
4.0	1.4	8
4.0	1.4	16
4.0	1.4	32
4.0	1.6	8
4.0	1.6	16
4.0	1.6	32
4.0	1.8	8
4.0	1.8	16
4.0	1.8	32

Our results echo the trends from the Mase et al. (2013) and Mase (2017) studies. In general, the initial times of liquefaction based on the Mase (2017) study under a vibration frequency of 1.8 Hz with 8, 16, and 32 seconds of vibration time are similar to this study results, especially under the same frequency and vibration times. For 8 seconds of shaking, the Mase (2017) study tended to result in longer initial times at accelerations of 3 m/s<sup>2</sup>, but slightly shorter initial times at accelerations of 3.5 m/s<sup>2</sup> and 4 m/s<sup>2</sup>. A similar trend was also found with vibration times of 16 and 32 seconds. This indicates that Imogiri sand tends to be liquefied in a shorter time compared to Watu sand, especially under a vibration frequency of 1.8 Hz.

The comparison to the Mase et al. (2013) study of a vibration frequency of 1.6 Hz and a vibration time of 32 seconds also shows a trend similar to that obtained in the Mase (2017) study. The initial liquefaction time of Watu sand tends to be longer than that of Imogiri sand under a vibration frequency of 1.6 Hz and a vibration time of 32 seconds. This may be caused by the soil properties that influence liquefaction. In general, the soil properties of both sands are quite similar. However, there are the exceptions due to the granular gradation of both sands. The uniformity coefficient ( $C_u$ ) of Watu sand is about 3.4, whereas for Imogiri sand, it is 1.75. Furthermore, the curvature coefficients ( $C_c$ ) of Watu sand and Imogiri sand are about 1.4 and 0.875, respectively. From both coefficients, it can be concluded that the Watu sand gradation is better than Imogiri sand, since the values are closer to the standard value for good gradation sand, i.e.,  $C_u > 6$  and  $1 < C_c < 3$ . During shaking, pore pressure tended to build up easily in more uniformly sandy soil; therefore the initial time of liquefaction for Watu sand tended to be longer than for Imogiri sand, especially under higher acceleration.

### 4.3. The Time to Start Dissipation

Figure 8 shows the time to start dissipation. In general, vibration time influenced the dissipation of pore water pressure. A longer vibration time and a higher dynamic load generated longer initial dissipation times. The longer vibration time maintains pore water pressure at the liquefaction threshold. Besides, the higher dynamic load possibly generates a shorter initial time of liquefaction. When this load was applied for a longer time, the initial time of pore water pressure dissipation tended to be longer.

The trends in this study also are similar to the trends in the Mase et al. (2013) and Mase (2017) studies, especially under the frequency of 1.8 Hz for the vibration times of 8, 16, and 32 seconds, and under 1.6 Hz for the vibration time of 32 seconds, respectively. In general, the time to start dissipation in the Mase (2017) study was slightly higher than the result obtained from the acceleration of  $4 \text{ m/s}^2$  and the vibration frequency of 1.8 Hz applied for a vibration time of 8 seconds, whereas under acceleration of 3 and  $3.5 \text{ m/s}^2$ , the time to start dissipation of Watu sand was higher. For the vibration times of 16 and 32 seconds, the time to start dissipation was shorter than in the Mase (2017) study. The comparison to a 1.6 Hz vibration frequency applied for 32 seconds in the Mase et al. (2013) study showed that the time to start dissipation tended to be longer than this study result, especially at an acceleration of 3, whereas at 3.5 and  $4 \text{ m/s}^2$ , the initial times of pore pressure dissipation for both sands were close. Based on the comparisons, it can be said that the time to start dissipation for Imogiri sand tends to be longer than that for Watu sand, especially under a vibration frequency of 1.8 Hz and vibration times of 16 and 32 seconds. Meanwhile, under dynamic load applied at a vibration frequency of 1.6 Hz for 32 seconds, the time to start dissipation for Watu sand is consistent with that for Imogiri sand, especially at accelerations of 3.5 and  $4 \text{ m/s}^2$ . In keeping with the explanation given in the previous section, the soil properties seem to play a role in pore pressure dissipation. After shaking, both sands tend to compact at the same values of relative density. When the load stopped, the soil granules had snuggled into each other. This would result in the pore water, which was not easily drained; therefore, when the load stopped, the time to start dissipation is similar.

### 4.4. Liquefaction Duration

Liquefaction duration due to the dynamic load is presented in Figure 9. In this study, liquefaction duration was estimated from the difference between initial time of liquefaction and initial time of pore pressure dissipation. In Figure 9, the shortest liquefaction duration is about 6 seconds, which occurs under an acceleration of  $3 \text{ m/s}^2$  and a vibration frequency of 1.4 Hz, and the longest liquefaction duration is about 35 seconds, under a dynamic load of  $4 \text{ m/s}^2$  and  $f$  of 1.8 Hz. The result shows that the dynamic load and vibration time strongly influence the liquefaction duration. Liquefaction that occurs in a short time and starts to dissipate over a longer time results in a longer liquefaction duration.

The increase in the percentage of the liquefaction duration is presented in Figure 10. By way of explanation, the calculation of this percentage for an acceleration of  $3.5 \text{ m/s}^2$  is the difference in liquefaction duration under 3 and  $3.5 \text{ m/s}^2$ , divided by the liquefaction duration of the initial test, which in this case was  $3 \text{ m/s}^2$ . Therefore, the percentage would be 50%, simply derived from  $(2 \times 100 / 4)\%$ , for  $3.5 \text{ m/s}^2$ , and 125% for  $4 \text{ m/s}^2$ .

In general, the increase in liquefaction duration on all tests varied from 9 to 163%. The comparison was performed for the first test on each loading criterion. For example, the liquefaction durations that resulted under a vibration frequency of 1.4 Hz applied for 8 seconds with accelerations of 3, 3.5, and  $4 \text{ m/s}^2$  were 4, 6, and 9 seconds, respectively. In general, a lower vibration frequency tended to result in a larger increase in the percentage of liquefaction duration. However, when the duration increased, the increment in the percentage tended to

decrease. Generally, the results indicated that the increase in dynamic load applied for 8 seconds tended to result in a significant increment beyond that due to the previously applied load. This can explain why, for example, under an acceleration of  $3 \text{ m/s}^2$  and a vibration frequency of 1.4 Hz, the liquefaction duration is about 4 seconds, but when the acceleration increases to  $3.5 \text{ m/s}^2$ , the liquefaction duration is about 8 seconds. Therefore, the percentage tends to increase greatly.

The results also reflect the fact that Watu sand granules are quite sensitive to the vibration frequency of 1.4 Hz, since the vibration resulting from the frequency tends to critically compact the soil deposit. This means that an acceleration of  $3 \text{ m/s}^2$  arranges sand granules, but does not fully compact them, and it results in a shorter liquefaction duration, since the pore pressure generated is not large. When an acceleration of  $3.5 \text{ m/s}^2$  is applied, sand granules are more significantly compacted and the pore pressure is larger than for the previous one (acceleration of  $3 \text{ m/s}^2$ ). This also happens when an acceleration of  $4 \text{ m/s}^2$  is applied. The vibration time also influences this percentage; longer time tends to result in a lower percentage. This is because at the longer duration, the pore pressure increases to the maximum value to generate liquefaction, i.e., pore pressure equal to or larger than the effective stress. At that moment, the increase in liquefaction duration is not significantly different from that under the previously applied load. Therefore, the increase in the percentage of liquefaction duration tends to decrease proportionately to the increase in vibration time. Based on these results, it can be said that 8 seconds shaking is the critical duration for the soil to be compacted, and this influences the increase in the percentage of the liquefaction duration.

Comparison to the previous studies also showed a similar trend in results. The comparison to the Mase (2017) study under a vibration frequency of 1.8 Hz applied for 8 seconds showed that the liquefaction duration of Imogiri sand tended to be longer than for Watu sand, especially under an acceleration of  $4 \text{ m/s}^2$ . However, under accelerations of 3 and  $4 \text{ m/s}^2$ , the liquefaction durations of Imogiri sand were shorter than those of Watu sand. For the other two vibration times, the liquefaction duration of Imogiri sand was longer than for Watu sand. The percentage increase in the liquefaction duration for Watu sand tended to be higher, especially at an acceleration of  $4 \text{ m/s}^2$  applied for 8 seconds. For a vibration time of 16 seconds, the liquefaction duration percentage was consistent with each other. The increase in the percentage of liquefaction duration of Imogiri sand tended to be lower than for Watu sand for the all accelerations with a vibration frequency of 1.8 Hz applied for 32 seconds. The comparison to the Mase et al. (2013) study for a vibration time of 32 seconds and a frequency of 1.6 Hz showed that the liquefaction duration of Watu sand was shorter than that of Imogiri sand under an acceleration of  $3 \text{ m/s}^2$ , whereas under an acceleration of 3.5 and  $4 \text{ m/s}^2$ , both Watu and Imogiri sands showed similar liquefaction durations. In term of an increase in duration as a percentage, Imogiri sand under a vibration frequency of 1.6 Hz tended to yield a smaller increase in duration as a percentage than did Watu sand.

#### 4.5. Maximum $r_u$

Referring to the time histories of excess pore water pressure shown in Figures 5, 6, and 7,  $r_u \text{ max}$  under each dynamic load was calculated (Figures 11 and 12). In Figure 11, it can be observed that dynamic load and vibration time strongly influence the  $r_u \text{ max}$ . If higher dynamic loads are applied,  $r_u \text{ max}$  rises as well. Moreover, if the higher load is applied for a longer time,  $r_u \text{ max}$  tends to be larger. The higher dynamic load generates liquefaction in a short time and a higher  $r_u$ . The longer duration continuously gives the contribution of excess pore water pressure and supplies more generated excess pore water pressure thus increasing  $r_u$ .

The comparison to Mase et al. (2013) for a vibration frequency of 1.6 Hz applied for 32 seconds with various accelerations showed a similar trend to our results. In general, the



dynamic loads applied to Imogiri sand resulted in a lower excess pore pressure ratio than for Watu sand. For a vibration frequency of 1.8 Hz and various accelerations, our results were compared to those in the Mase (2017) study. In general, for 8 seconds' shaking, the maximum excess pore pressure ratio was higher than in the Mase (2017) study. A similar tendency was also observed for the various accelerations and frequencies applied for 16 seconds and 32 seconds. From the comparison of the results, it can be concluded that Watu sand under the same dynamic load with various accelerations and vibration frequencies tends to result in a larger  $r_u$  than does Imogiri sand.

In general, pore pressure tends to build up easily in uniform sandy soil. It may affect the initial liquefaction, pore pressure dissipation, and liquefaction duration. However, as a result of pore pressure buildup, the soil tends to be compacted faster. When it is compacted, the pore pressure still increases by a small amount. This is because the released energy can not release the much larger pore pressure due to the obstruction of water, which is caused by the decrease in the permeability (due to shaking compaction). As a result, the incremental pore water pressure is not significant and the excess pore pressure ratio does not increase greatly. Therefore, in Figures 4, 5, and 6, when liquefaction was reached, the tendency of  $r_u$  after the load is stopped, was relatively flat, which means that the pore pressure ratio was not very significant. When the generated amount of  $r_u$  was smaller, the excess pore water pressure was smaller too.

**4.6. Required Time to Generate  $r_u$  max**

Figure 12 presents the time required to generate  $r_u$  max. Generally, higher dynamic loads combined with longer vibration times tend to result in higher  $r_u$  max. The dynamic loads together with a longer vibration time also influence the time to start liquefaction. A higher dynamic load results in liquefaction in a short time, compared with the lower dynamic load. A longer vibration time tends to result in a longer time to generate  $r_u$  max. A dynamic load applied over a longer time can generate a higher  $r_u$ .  $r_u$  max due to a higher dynamic load applied for a longer time is higher than  $r_u$  max resulting from a higher dynamic load applied for shorter time.

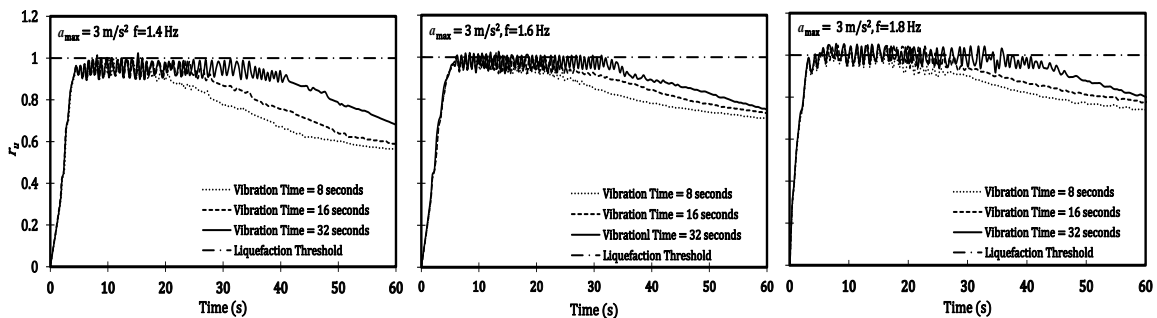


Figure 4  $r_u$  for an acceleration of  $3 \text{ m/s}^2$

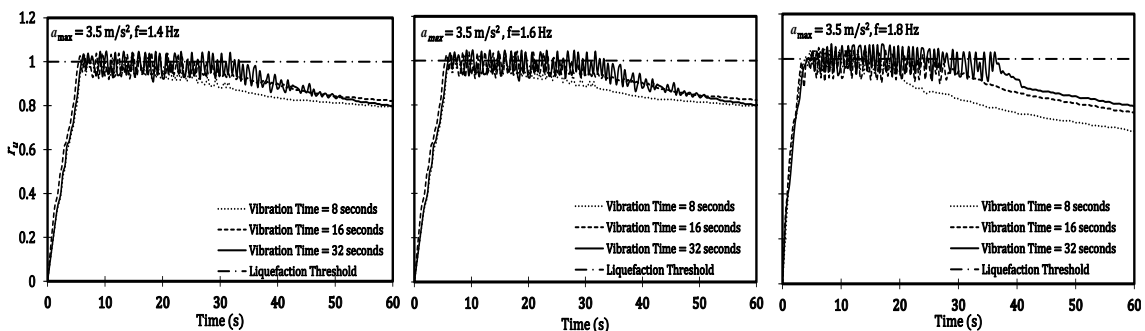


Figure 5  $r_u$  for an acceleration of  $3.5 \text{ m/s}^2$

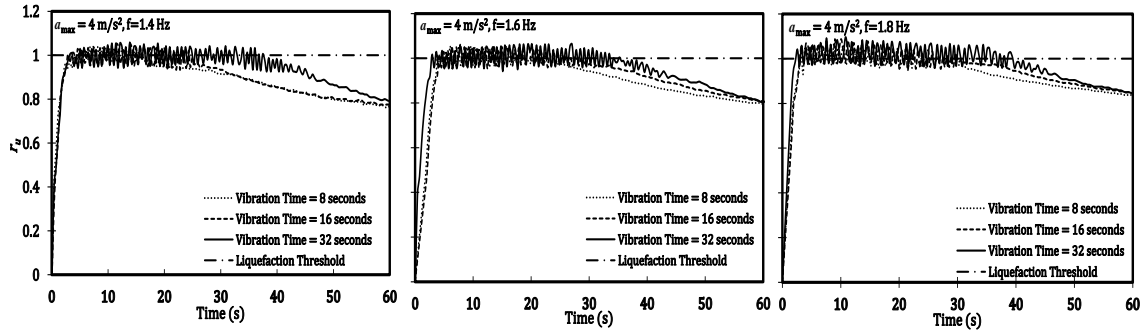


Figure 6  $r_u$  for an acceleration of  $4 \text{ m/s}^2$

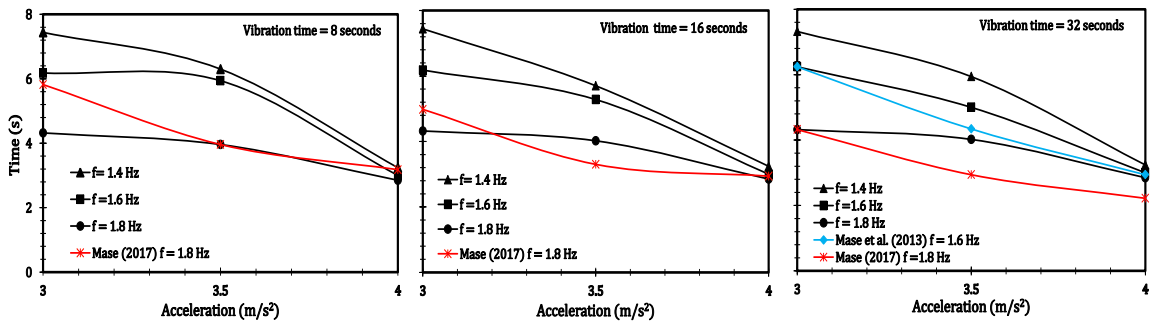


Figure 7 The time to start liquefaction for variations in vibration time

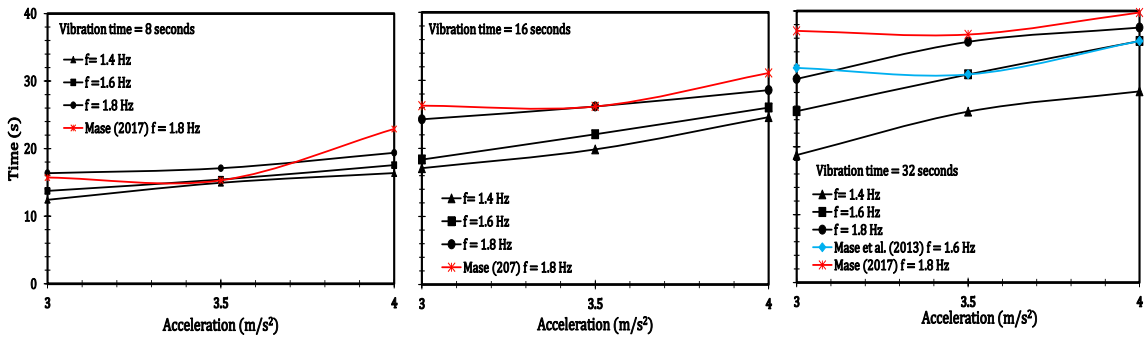


Figure 8 The time to start dissipation

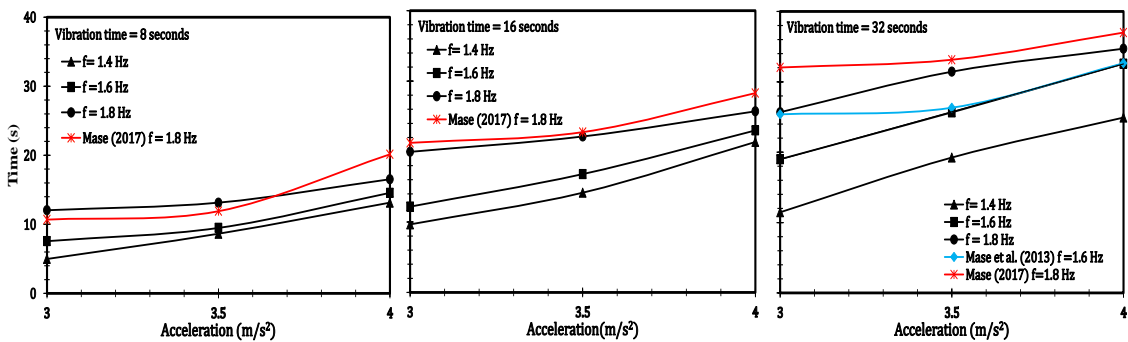


Figure 9 Liquefaction duration

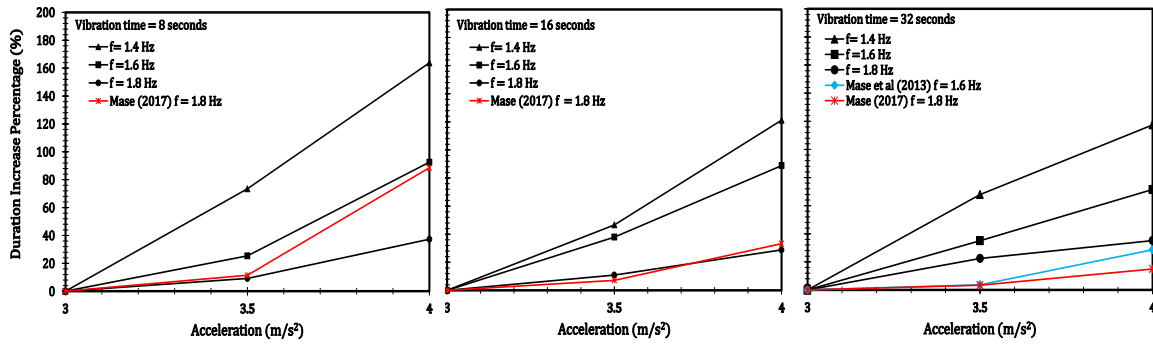


Figure 10 Increase (as a percentage) in liquefaction duration

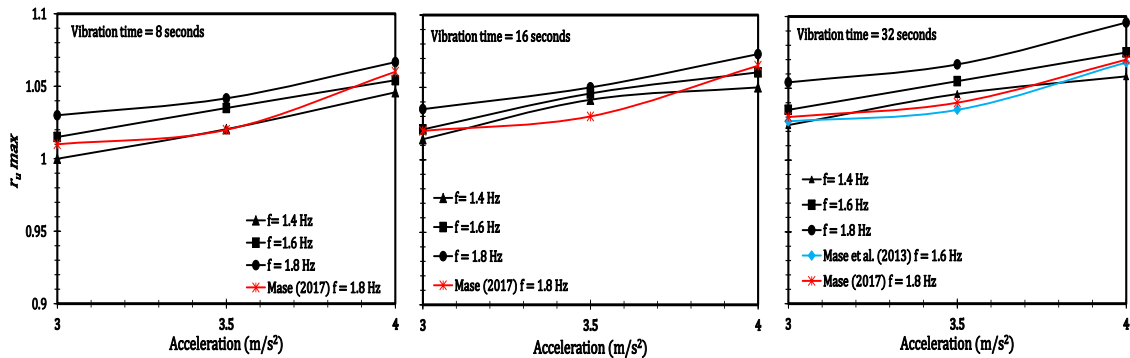


Figure 11  $r_{u, max}$

**4.7.  $r_u$  Versus Time under Secondary Vibration**

After all tests were conducted, all dynamic loads were applied again to the soil deposit in the container. This process was initiated by measuring the actual density after shaking, and continued by secondary vibration. The initial excess pore water pressure was measured as in the first test. This secondary test was expected to reveal the possibility of re-liquefaction of the soil deposit after the primary shaking. The excess pore water pressures in these tests are shown in Figures 13, 14, and 15. Figure 13 presents the test results of re-shaking for an acceleration of 3  $m/s^2$ . Based on the results, it can be observed that liquefaction did not occur due to re-shaking under the same dynamic load as was applied in first test. The same trend is also observed for an acceleration of 3.5  $m/s^2$  (Figure 14) and 4  $m/s^2$  (Figure 15). The results indicate that there is an increment in soil stiffness due to the primary shaking. The primary shaking compacted the soil, which decreased the void ratio of soil and increased soil resistance. This increment also influences the soil density and increases the soil effective stress. Therefore, the larger dynamic load must be applied to produce the extra energy for generating the liquefaction again. This observation was made shortly after the first dynamic load was applied. Therefore, the effect of dynamic load on the liquefied soil and the possibility of re-liquefaction in long term resting cannot be estimated.

**4.8. Reduction in  $r_u$**

$r_{u, max}$  under the main dynamic loads and the secondary dynamic loads were compared to determine the percentage of  $r_u$  reduction (Table 3). In general, there were reductions in  $r_u, max$  of about 20–25%. However, there were no significant differences in the reduction of  $r_u$  under any dynamic loads. As discussed in the previous section, primary shaking increases the effective soil stress of the soil deposit. In other words, the required excess pore water pressure to generate re-liquefaction should be larger as well. The primary shaking also arranges the soil grains more compactly, so that greater pore water pressure is not generated. The impact is that

the excess pore water pressure is not able to decrease the effective soil stress significantly. Therefore, in these cases, liquefaction is not able to occur for the second time.

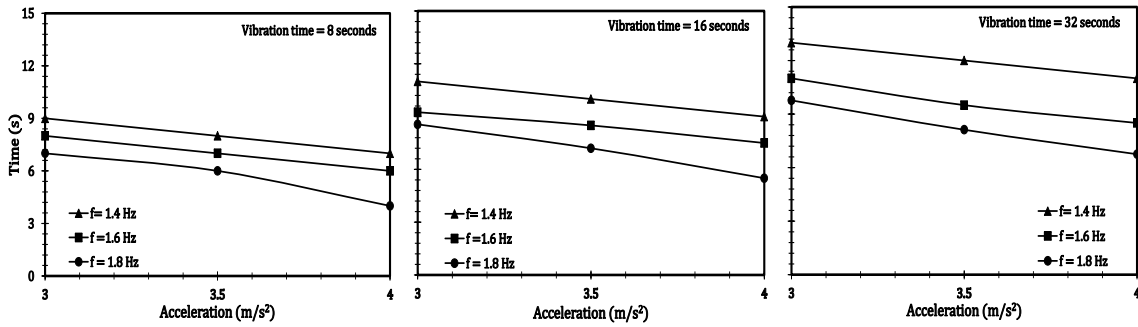


Figure 12 Time required to generate  $r_u \max$

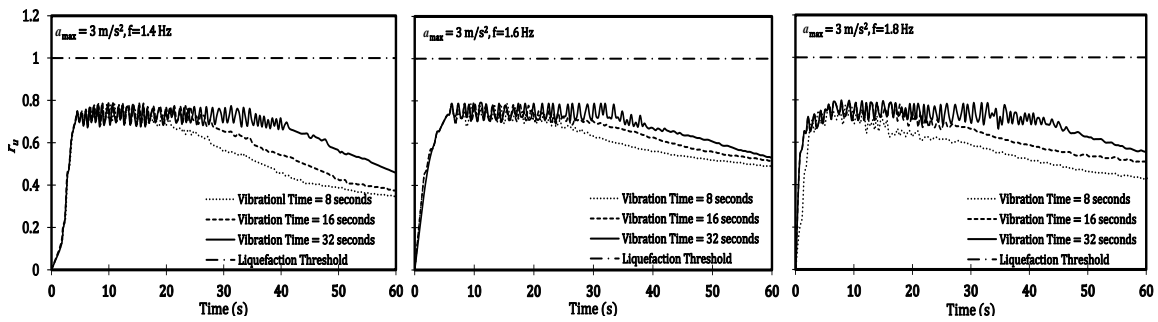


Figure 13  $r_u$  under an acceleration of  $3 \text{ m/s}^2$  (secondary shaking)

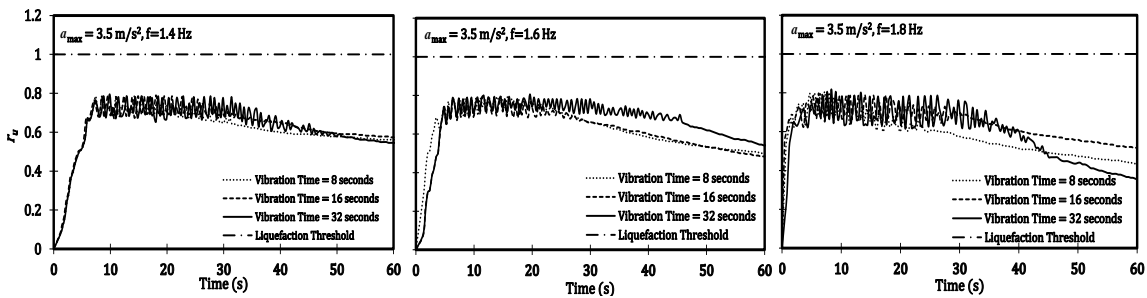


Figure 14  $r_u$  under an acceleration of  $3.5 \text{ m/s}^2$  (secondary shaking)

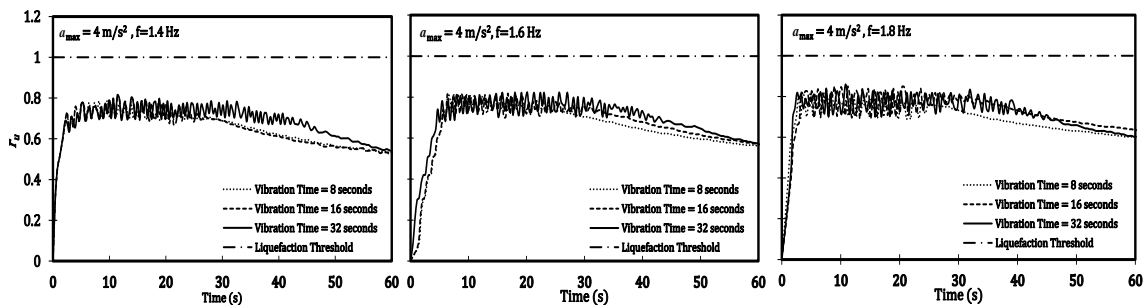


Figure 15  $r_u$  under an acceleration of  $4 \text{ m/s}^2$  (secondary shaking)

Table 3 Reduction in  $r_u$  max

Dynamic Load	Reduction of $r_u$ (%)		
	Vibration time of 8 s	Vibration time of 16 s	Vibration time of 32 s
$a = 3 \text{ m/s}^2$ $f = 1.4 \text{ Hz}$	23.9	23.5	24.1
$a = 3 \text{ m/s}^2$ $f = 1.6 \text{ Hz}$	24.6	23.1	23.9
$a = 3 \text{ m/s}^2$ $f = 1.8 \text{ Hz}$	24.5	22.9	23.8
$a = 3.5 \text{ m/s}^2$ $f = 1.4 \text{ Hz}$	23.3	24.0	24.1
$a = 3.5 \text{ m/s}^2$ $f = 1.6 \text{ Hz}$	23.3	23.7	23.6
$a = 3.5 \text{ m/s}^2$ $f = 1.8 \text{ Hz}$	22.9	22.3	23.3
$a = 4 \text{ m/s}^2$ $f = 1.4 \text{ Hz}$	22.8	22.8	23.1
$a = 4 \text{ m/s}^2$ $f = 1.6 \text{ Hz}$	22.8	22.9	23.5
$a = 4 \text{ m/s}^2$ $f = 1.8 \text{ Hz}$	22.5	21.1	21.6

## 5. CONCLUSION

According to a preliminary investigation of soil liquefaction based on grain size criteria, Watu sand is indicated as being very vulnerable to liquefaction. The results also indicate that liquefaction can potentially happen under applied dynamic loads. This is shown by the value of  $r_u$ , which was higher than one on each test. The  $r_u$  was strongly influenced by dynamic load and vibration time. This is clearly seen at each stage by important measures of liquefaction, i.e., initial time of liquefaction, initial time of pore water pressure dissipation, and liquefaction duration. The dynamic load and vibration time also play a role in determining  $r_u$  max. However, the vibration time does not significantly influence the time required to generate  $r_u$  max.

The primary shaking actually influences the soil stiffness. This is obvious in the generated pore excess pore water pressure under a secondary dynamic load. This indicates that the first shaking successfully increases the soil density.

The reduction in  $r_u$  in this study was about 20 to 25%. This indicates that the impact of accelerations of 3 to 4  $\text{m/s}^2$  with variations in vibration frequency and vibration time do not produce a significant effect in generating re-liquefaction. In general, the results are consistent with those of previous studies that performed tests of liquefaction in the same region as did this study, i.e., southern Yogyakarta.

## 6. ACKNOWLEDGEMENT

The authors are grateful to Balai Pelestarian Cagar Budaya (BPCB) (Cultural Heritage Preservation Agency) of Prambanan Temple for the shaking table equipment.

## 7. REFERENCES

- Casagrande, A., 1936. Characteristics of Cohesionless Soils Affecting the Stability of Slopes and Earthfills, *Boston Society of Civil Engineers*, Volume 23, pp. 257–276
- Chang, F.K., Krinitzsky, E.L., 1977. Duration, Spectral Content, and Predominant Period of Strong Motion Earthquake Records from Western United States. *Miscellaneous Paper 5-73-1, US Army Corps of Engineers Waterways Experiment Station*, Vicksburg, Mississippi, USA
- Fathani, T.F., Adi, A.D., Pramumijoyo, S., Karnawati, D. in: Karnawati, D., Pramumijoyo, S., Anderson, R., Hussein, S. (Eds.), 2008. *The Determination of Peak Ground Acceleration at Bantul Regency*, Yogyakarta Province, Indonesia, STAR Publishing Company Inc., California, pp. 7-1 to 7-15
- Gupta, M.K., 1977. *Liquefaction of Sands during Earthquakes*, Ph.D. Thesis, University of Roorkee, Roorkee, India

- Iwasaki, T., Tokida, K.I., Tatsuoka, F., Watanabe, S., Yasuda, S., Sato, H., 1982. Microzonation for Soil Liquefaction Potential using Simplified Methods. *In: Proceedings of the 3rd International Earthquake Microzonation Conference, Seattle, 28 June -1 July, USA*, pp. 1319–1330
- Komaji, R.F., 2014. *Experimental Study of Static Loading Effect to Liquefaction Potential by using Shaking Table Equipment*, Master's Thesis, Gadjah Mada University, Yogyakarta, Indonesia
- Kusumawardhani, R., 2014. *Liquefaction Variable based on Experimental Test of Very Low Frequency in Clean Sand*, Ph.D. Thesis, Gadjah Mada University, Yogyakarta, Indonesia
- Laia, B., 2014. *The Effect of Sand Relative Density to Liquefaction Potential in Opak River Pleret*, Master's Thesis, Gadjah Mada University, Yogyakarta, Indonesia
- Mase, L.Z., 2013. *Analysis of Liquefaction Potential of Opak Imogiri River (Experimental Study and Empirical Analysis)*, Master's Thesis, Gadjah Mada University, Yogyakarta, Indonesia
- Mase, L.Z., 2017. Experimental Liquefaction Study of Southern Yogyakarta using Shaking Table, *Teknik Sipil (Jurnal Teoritis dan Terapan Bidang Rekayasa Sipil)* ITB, Volume 24(1), pp. 11–18
- Mase, L.Z., Fathani, T.F., and Adi, A.D., 2013. Experimental Study of Liquefaction Potential in Opak River Imogiri, Yogyakarta. *In: Proceedings of the 17<sup>th</sup> Annual Scientific Meeting of the Indonesian Geotechnical Engineering Society, Jakarta, 13-14 November, Indonesia*, pp. 199–205
- Singh, H.P., Maheswari, B.K., Saran, S., 2008. Liquefaction Behavior of the Solani Sand using Small Shake Table, *In: Proceedings of The 12<sup>th</sup> International Conference of the International Association for Computer Method and Advances in Geomechanics, Goa, 1-6 October, India*, pp. 2797–2804
- SNI 03-1726-2010, 2010. *Standard of Earthquake Resistance Design for Building*, National Standardization Agency, Jakarta, Indonesia
- Tsuchida, H., 1970. Prediction and Countermeasure Against Liquefaction in Sand Deposits. *Abstract of the Seminar of the Port and Harbour Research Institute*, Volume 1.3. pp.1–3, Japanese Ministry of Transport, Yokosuka, Japan
- Yogatama, B.A., Fathani, T.F., 2013. Liquefaction Potential Analysis on Bantul Regency and Yogyakarta City Area. *In: Proceedings of the 17<sup>th</sup> Annual Scientific Meeting of the Indonesian Geotechnical Engineering Society, Jakarta, 13-14 November, Indonesia*, pp. 206–211